Silicate Nanotubes

Thermally Stable Silicate Nanotubes**

*Xun Wang, Jing Zhuang, Jun Chen, Kebin Zhou, and Yadong Li**

For many years, intense research has focused on new types of silicates with tunable pore sizes because of their great potentials in many areas, such as selective catalysis, molecular sieves, and gas adsorption and separation.[1–9] Zeolites with pore diameters of 3–10 Å (roughly the same size as small molecules)[1–2] have found wide industrial application, however their relatively small pore sizes deny access to large molecular and/or bulky reactants and thus limit their further use in fine chemical and pharmaceutical industries. Recent progress in solving this problem has been made through the development of mesoporous silica[3–6] and non-silica[7–9] materials (MCM-41, etc) with pore diameters in the order of nanometers, however, compared with zeolites, mesoporous materials usually suffer from poor thermal and/or hydrothermal stability due to the amorphous nature of the mesoporous walls, which have limited their practical applications. Thus new porous materials require a combination of stability and appropriate size distributions to meet practical requirements, which still remains a challenge to materials scientists worldwide. Herein we demonstrate a new form of porous silicate nanotubes with excellent thermal stability (comparable to zeolites) and uniform pore sizes distributions in the order of nanometers, which may find wide application in gas adsorption/separation and catalysis.

The general synthesis of porous silicates nanotubes (such as main-group-metal and transition-metal silicates) is based on a hydrothermal synthetic process in a mixed water/ethanol solvent system. Under optimal solvent ratio and basicity conditions, a series of silicate nanotubes can be obtained. Here we demonstrate copper and magnesium silicates as representative examples. The phase purity of the samples has been characterized on a Bruker D8-Advance X-ray powder diffractometer with $Cu_{K\alpha}$ radiation ($\lambda = 1.5418$ Å). Figure 1 shows the XRD patterns of copper and magnesium silicates. All of the reflection patterns in Figure 1a can be readily indexed to that of a pure hexagonal phase of $Mg_3Si_2O_5(OH)_4$ with lattice constants $a = 5.33$ and $c = 7.269$ Å (JCPDS no. 82–1838) while the main peaks centered at $2\theta = 20.04$, 30.61, 36.07, 56.17, and 62.15° in Figure 1c can be indexed to the $CuSiO_3{\cdot}2H_2O$ phase (JCPDS no. 11-0322). The apparent broadening of these peaks indicates the small crystal sizes of the obtained nanotubes. Other silicates have been characterized by means of XRD and all the information indicates that as-obtained silicate nanotubes usually have distinctive clay-type structures with silicon to oxygen ratios of 1:2.5 within the layers.[10–11] Due to the excellent ion-exchange characteristics of layered silicates, cations residing between the layers can be further replaced, which make these nanotubes ideal candidates as molecular sieves.

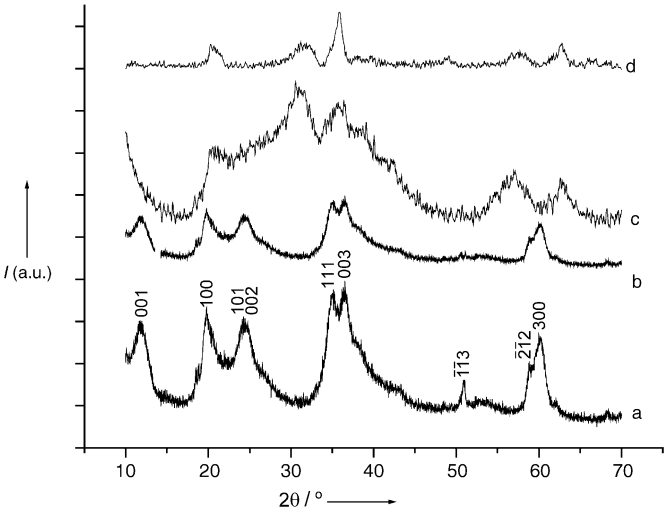

Figure 1. X-ray diffraction patterns of a) $Mg_3Si_2O_5(OH)_4$ nanotubes; b) $Mg_3Si_2O_5(OH)_4$ nanotubes after calcination for 12 h at 600 °C; c) $CuSiO_3{\cdot}2H_2O$ nanotubes; d) $CuSiO_3{\cdot}2H_2O$ nanotubes after calcination for 12 h at 600 °C. I = intensity.

[*] Dr. X. Wang, J. Zhuang, Dr. K. Zhou, Prof. Y. Li
Department of Chemistry
Tsinghua University
Beijing, 100084 (P.R. China)
Fax: (+86) 10-6278-8765
E-mail: ydli@mail.tsinghua.edu.cn
Prof. J. Chen
Institute of New Energy Material Chemistry
Nankai University
Tianjin 300071 (P.R. China)

[**] This work was supported by NSFC (50372030, 20025102, 50028201, 20151001), the Foundation for the Author of National Excellent Doctoral Dissertation of P.R. China and the state key project of fundamental research for nanomaterials and nanostructures.

Supporting information for this article is available on the WWW under http://www.angewandte.org or from the author.

 DOI: 10.1002/ange.200353507

TEM analysis has provided further insight into the microstructural details of these nanotubes. As shown in Figure 2, all the samples dispersed on to the TEM copper grids have uniform nanotube morphologies with open ends,

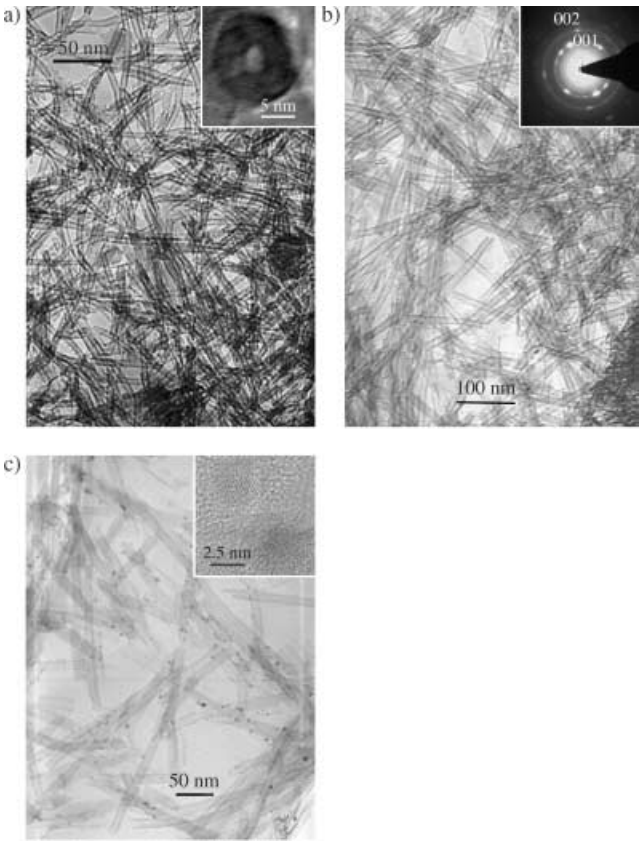

Figure 2. a) TEM images of $CuSiO_3 \cdot 2H_2O$ nanotubes; b) TEM images of $Mg_3Si_2O_5(OH)_4$ nanotubes (inset: electron diffraction patterns taken from a bundle of $Mg_3Si_2O_5(OH)_4$ nanotubes); c) TEM images of Pd nanoparticles supported on $Mg_3Si_2O_5(OH)_4$ nanotubes (inset: HRTEM images of Pd nanoparticles with diameters of $\approx$2.5 nm.

which enable them to have potential application in gas absorption/separation and catalysis. For different interlayer cations, the silicate nanotubes have different diameters, possibly due differences in the interaction between layers and the subsequent difference in the rigidity of the silicate sheets; for example, copper silicate nanotubes have diameters of 8–10 nm and lengths up to hundreds of nanometers (Figure 2a), while those of magnesium (Figure 2b), calcium, and cadmium silicates (see Supporting Information) have diameters of 15–20 nm and lengths up to 1 μm. The inset in Figure 2a shows an individual copper silicate nanotube parallel to the electron beam, from which the hollow structural features can be clearly seen with an inner diameter of $\approx$2 nm and an outer diameter of $\approx$10 nm. Electron diffraction patterns, taken from bundles of nanotubes, indicate that the nanotubes are crystalline (the inset in Figure 2b shows the ED pattern taken from bundles of magnesium silicates nanotubes, which can be indexed to layered hexagonal $Mg_3Si_2O_5(OH)_4$. Together with the XRD results, the ED information provides further evidence that the formation of these silicate nanotubes can be attributed to the intrinsic layer structures of clay-type silicates. However, in contrast to the well-known WS_2 and carbon nanotubes,[12–17] which have symmetric layer structures, the growth of these nanotubes is believed to be based on asymmetry along the *c* axis of the layered metal silicate (see Supporting information).[18,19] As potential catalyst supports, these silicate nanotubes have shown their ability in stabilizing and supporting noble-metal nanoparticles. Through a water/ethanol reflux method, uniform noble-metal nanoparticles supported on silicate nanotubes can be easily prepared, and by altering the experimental parameters the diameters can be further tuned. Figure 2c shows typical images of well-dispersed uniform Pd nanoparticles with diameters of 2–3 nm supported on magnesium silicates. HRTEM analysis (Figure 2c, inset) show that the nanocrystals are highly crystalline, which enhances their potential for applications in catalytic fields.

To investigate the statistical data that derive from these nanotubes (such as surface area and pore-size distributions), which are critical for practical applications, BET analysis has been carried out. Figure 3 shows nitrogen adsorption/desorption isotherms of copper and magnesium silicate nanotubes. These isotherms can be categorized as type IV with a distinct hysteresis loop. The BET surface area is calculated to be about 200 $m^2 g^{-1}$ for the $CuSiO_3 \cdot 2H_2O$ nanotubes and 320 $m^2 g^{-1}$ for the $Mg_3Si_2O_5(OH)_4$ nanotubes. Barrett–Joyner–Halenda calculations for the pore-size distribution, derived from desorption data, reveal a narrow distribution for the $CuSiO_3 \cdot 2H_2O$ samples centered at 2–3 nm (Figure 3a, inset) and $Mg_3Si_2O_5(OH)_4$ samples centered at 12 nm (Figure 3b, inset), which coincide well with the XRD and TEM results of the samples.

Thermal and hydrothermal stability are important factors that will greatly influence the working performance of catalysts. Based on our experimental results, these nanotubes show good thermal and hydrothermal stability. In addition, after calcination at 600 °C for 12 h, or at 800 °C for 12 h in flowing water vapor, or treating in boiling water for 240 h, the main peaks in XRD patterns show little change and TEM characterizations indicate that the tubular structures have been preserved. Meanwhile, the BET data usually shows only a small reduction (for example, the surface area of the magnesium silicate nanotubes is reduced to 290–300 $m^2 g^{-1}$), further evidence of the good thermal stability of these nanotubes.

The large surface areas, narrow size distributions, and excellent thermal stability combine to enhance the potential applications of these novel nanotubes. Furthermore, their reversible hydrogen storage[20–24] and catalytic properties can be examined.[25,26]

The complete PCT (pressure–composition–temperature) curves of $CuSiO_3 \cdot 2H_2O$ and $Mg_3Si_2O_5(OH)_4$ nanotubes at 25 °C are shown in Figure 4. The hydrogen concentration in the $CuSiO_3 \cdot 2H_2O$ nanotubes is 1.1 wt % at 10 atm, 1.6 wt % at 20 atm, and 1.8 wt % at 40 atm (Figure 4b), a value higher than that of any of the reported Si-related materials (such as silicates, zeolites, and MCM-41 materials etc).[24] Further treatment can lead to an increase in hydrogen storage capacity, for example, when doped with Pd nanoparticles

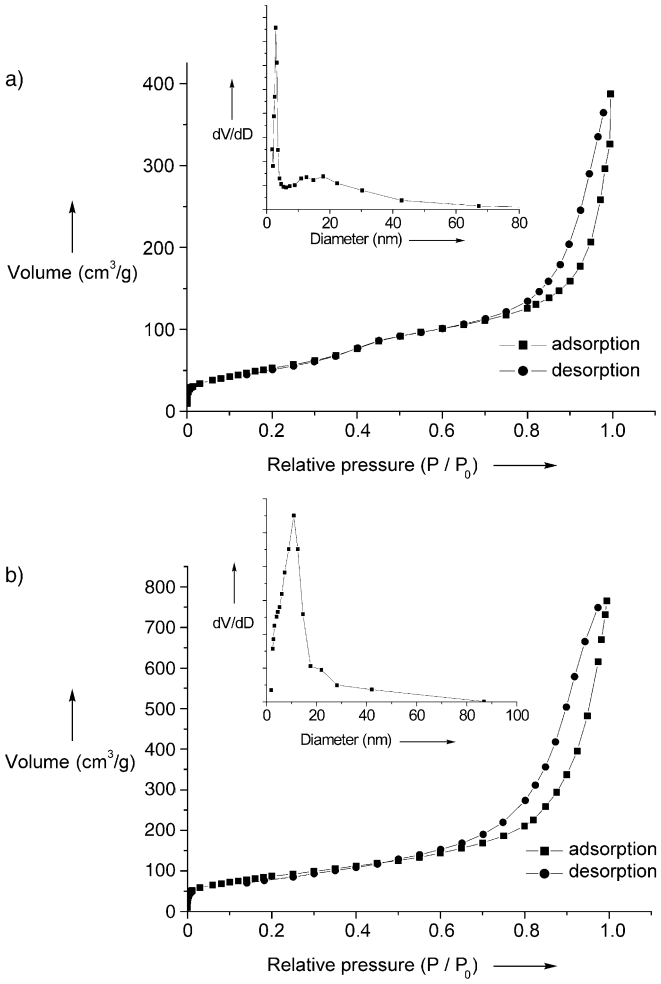

Figure 3. a) N_2 adsorption/desorption isotherm of $CuSiO_3 \cdot 2H_2O$ nanotubes (inset: pore-size distribution curve obtained from the desorption data); b) N_2 adsorption/desorption isotherm of $Mg_3Si_2O_5(OH)_4$ nanotubes (inset: pore-size distribution curve obtained from the desorption data).

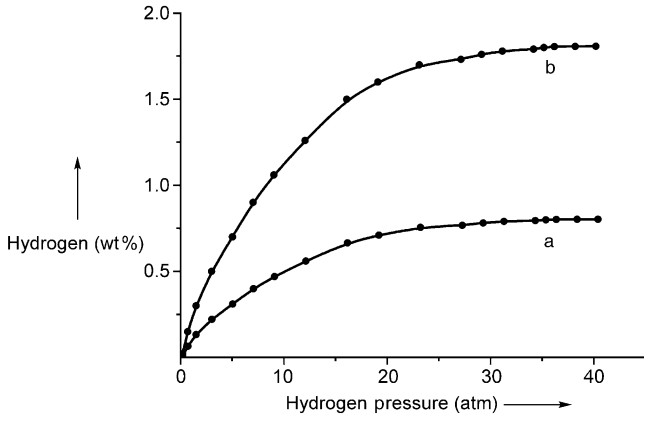

Figure 4. PCT curves for the hydrogen storage of a) $Mg_3Si_2O_5(OH)_4$ and b) $CuSiO_3 \cdot 2H_2O$ nanotubes at 25 °C.

(1%) the capacity of $CuSiO_3 \cdot 2H_2O$ nanotubes can reach 2.0% at room temperature and 40 atm, which may be attributed to the interaction between H atoms and the surface of the Pd nanoparticles. The exact understanding of the hydrogen storage and gas adsorption in these silicates nanotubes, including the absorption modes and adsorption sites, is still under investigation. Nevertheless, these nanotubes have shown their potential in hydrogen storage and gas adsorption (e.g., CO and CH_4) and separation fields.

The silicate nanotubes have also proved to be ideal catalyst supports. For example, with a Pd loading capacity of 0.1 wt%, the $Mg_3Si_2O_5(OH)_4$ nanotube/Pd catalysts show excellent catalytic activity for the complete catalytic oxidation of CO and C_2H_6 at $\approx$150 °C, a rather low temperature that is attractive for the treatment of vehicle exhaust gases. From Figure 5, it can be seen that conversion occurs at a

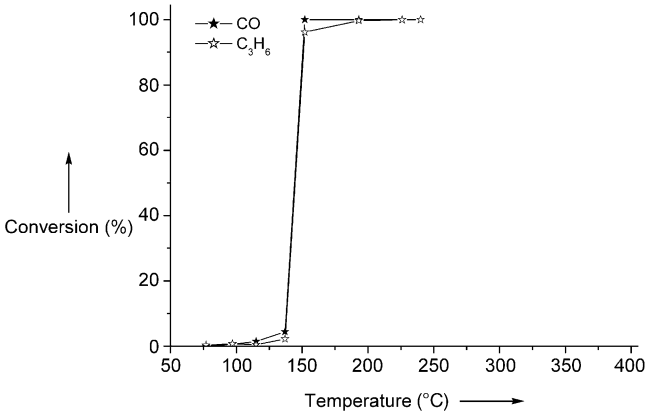

Figure 5. Catalytic oxidation of CO and C_3H_6 using Pd catalysts supported on $Mg_3Si_2O_5(OH)_4$ nanotubes.

temperature of $\approx$100 °C, and that the conversion rate gradually rises up to a temperature of $\approx$140 °C and then rises sharply to 100% at $\approx$150 °C, which indicates an effective low-temperature conversion process. Detailed studies concerning the catalytic mechanism and doping modes (for example, with Au-Pd bimetallic catalysts) affecting catalytic activity are in progress. Nevertheless, the novel properties exhibited by from this novel catalyst leads us to believe that silicate nanotubes will find application in various catalytic fields.

Experimental Section

The porous silicate nanotubes (both main-group-metal and transitional-metal silicates) were prepared by a hydrothermal process in a mixed water/ethanol solvent system. For example, $Cu(NO_3)_2 \cdot 3H_2O$ (0.5 g) was dissolved in a mixture of distilled water (5 ml) and ethanol (20 ml), into which ammonia solution was added to form a clear $[Cu(NH_3)_4]^{2+}$ solution. Then Na_2SiO_3 (5 ml, 0.5 M) was added to form a light-blue precipitate, which was transferred into a teflon-lined autoclave and hydrothermally treated at 180–200 °C for two days. The as-obtained precipitates were filtered and washed with distilled water to remove ions possibly remnaining in the final products, and dried at 70 °C in air. Slightly different conditions were employed for the magnesium silicate nanotubes: $Mg(NO_3)_2 \cdot 6H_2O$ (0.7 g) was dissolved in water/ethanol (5/30 mL), and Na_2SiO_3 (5 ml, 0.5 M) was used to form a white precipitate. Then NaOH (1.0 g) was added to adjust the basicity of the system. Series of other silicate nanotubes such as calcium, barium, cadmium, iron, and manganese silicates could also

be prepared based on the above procedures and the output can be readily kept above 95% based on the metal atoms.

Received: December 11, 2003 [Z53507]

Keywords: adsorption · heterogeneous catalysis · mesoporous materials · nanotubes · silicates

[1] A. Corma, *Chem. Rev.* **1997**, *97*, 2373 – 2419.
[2] R. M. Hazen, R. T. Downs, L. W. Finger, *Science* **1996**, *272*, 1769 – 1771.
[3] J. S. Beck, J. C. Vartuli, W. J. Roth, M. E. Leonowicz, C. T. Kresge, K. D. Schmitt, C. T.-W. Chu, D. H. Olson, E. W. Sheppard, S. B. McCullen, J. B. Higgins, J. L. Schlenkert, *J. Am. Chem. Soc.* **1992**, *114*, 10834 – 10843.
[4] D. Y. Zhao, J. L. Feng, Q. S. Huo, N. Melosh, G. H. Fredrickson, B. F. Chmelka, G. D. Stucky, *Science* **1998**, *279*, 548 – 552.
[5] Z. T. Zhang, Y. Han, L. Zhu, R. W. Wang, Y. Yu, S. L. Qiu, D. Y. Zhao, F. S. Xiao, *Angew. Chem.* 2001, *113*, 1298 – 1302; *Angew. Chem. Int. Ed.* **2001**, *40*, 1258 – 1262.
[6] F. S. Xiao, Y. Han, Y. Yu, X. J. Meng, M. Yang, S. Wu, *J. Am. Chem. Soc.* **2002**, *124*, 888 – 889.
[7] P. D. Yang, T. Deng, D. Y. Zhao, P. Y. Feng, D. Pine, B. F. Chmelka, G. M. Whitesides, G. D. Stucky, *Science* **1998**, *282*, 2244 – 2246.
[8] P. D. Yang, D. Y. Zhao, D. I. Margolese, B. F. Chmelka, G. D. Stucky, *Nature* **1998**, *396*, 152 – 155.
[9] T. Sun, J. Y. Ying, *Nature* **1997**, *389*, 704 – 707.
[10] R. R. Hao, X. Y. Fang, S. C. Niu, *Series of Inorganic Chemistry*, *Vol. 3*, Science Press, Beijing, **1998**, p. 212.
[11] D. T. Griffen, *Silicate crystal chemistry*, Oxford University Press, New York, **1992**.
[12] S. Iijima, *Nature* **1991**, *354*, 56 – 58.
[13] R. Tenne, L. Margulis, M. Genut, G. Hodes, *Nature* **1992**, *360*, 444 – 446.
[14] Y. Feldman, E. Wasserman, D. J. Srolovitz, R. Tenne, *Science* **1995**, *267*, 222 – 225.
[15] M. E. Spahr, P. Bitterli, R. Nesper, M. Müller, F. Krumeich, H. U. Nissen, *Angew. Chem.* **1998**, *110*, 1339 – 1342; *Angew. Chem. Int. Ed.* **1998**, *37*, 1263 – 1265.
[16] W. Tremel, *Angew. Chem.* **1999**, *111*, 2311 – 2315; *Angew. Chem. Int. Ed.* **1999**, *38*, 2175 – 2179.
[17] Y. D. Li, J. W. Wang, Z. X. Deng, Y. Y. Wu, X. M. Sun, D. P. Yu, P. D. Yang, *J. Am. Chem. Soc.* **2001**, *123*, 9904 – 9905.
[18] L. Pauling, *Proc. Natl. Acad. Sci. USA* **1930**, *16*, 578 – 582.
[19] G. Falini, E. Foresti, G. Lesci, N. Roveri, *Chem. Commun.* **2002**, 1512 – 1513.
[20] R. F. Service, *Science* **1999**, *285*, 682 – 685.
[21] M. S. Dresselhaus, I. L. Thomas, *Nature* **2001**, *414*, 332 – 337.
[22] N. L. Rosi, J. Eckert, M. Eddaoudi, D. T. Vodak, J. Kim, M. O'Keeffe, O. M. Yaghi, *Science* **2003**, *300*, 1127 – 1129.
[23] J. Chen, S. L. Li, Z. L. Tao, Y. T. Shen, C. X. Cui, *J. Am. Chem. Soc.* **2003**, *125*, 5284 – 5285.
[24] M. G. Nijkamp, J. E. M. J. Raaymakers, A. J. van Dillen, K. P. de Jong, *Appl. Phys. A* **2001**, *72*, 619 – 623.
[25] H. H. Kung, M. C. Kung, *Appl. Catal. A* **2003**, *246*, 193 – 196.
[26] G. A. Somorjai, Y. G. Borodko, *Catal. Lett.* **2001**, *76*, 1 – 5.

